Structure of GeS_2 glass: Spectroscopic evidence for broken chemical order

P. Boolchand and J. Grothaus
Physics Department, University of Cincinnati, Cincinnati, Ohio 45221

M. Tenhover, M. A. Hazle, and Robert K. Grasselli
Department of Research and Development, The Standard Oil Company (Ohio), 4440 Warrensville Center Road, Warrensville Heights, Ohio 44128

(Received 3 September 1985; revised manuscript received 6 January 1986)

Homogeneous melt-quenched $(Ge_{0.99}Sn_{0.01})_xS_{1-x}$ glasses in the glass-forming range $0<x<0.43$ have been studied by scanning calorimetry, Raman, and Mössbauer spectroscopy. At the stoichiometric composition $x=\frac{1}{3}$, two well-defined and chemically inequivalent ^{119}Sn sites are observed with the site intensity ratio $I_B/(I_A+I_B)=0.29(2)$. This ratio is found to vanish at $x=0.325$ and furthermore to change drastically with composition once $x>\frac{1}{3}$. This provides evidence for chemically correlated regions in GeS_2 glass which consist of two types of clusters—an A molecular cluster whose internal morphology is layerlike as in c-GeS_2 and a B molecular cluster whose building block consists of ethanelike $Ge_2(S_{1/2})_6$ units. The 340-cm^{-1} Raman band observed in GeS_2 glass is identified as having scattering contributions from both ordered bonds: A_1 from the symmetric stretch of $Ge(S_{1/2})_4$ units; and disordered bonds: A_{1g} mode from $Ge_2(S_{1/2})_6$ units; in the Ge-rich glasses $(x>\frac{1}{3})$, a third type of molecular cluster, C, is populated. The internal morphology of the C cluster resembles that of c-GeS and it consists of double layers. The 250-cm^{-1} Raman band, whose strength is correlated to the Mössbauer C sites, is identified as a double-layer breathing mode. The molecular structures of GeS_2 and $GeSe_2$ glasses are compared and contrasted.

I. INTRODUCTION

Infrared reflectance and Raman spectroscopy provide, in principle, rich structure information on network glasses. Decoding these vibrational spectra is straightforward only when narrow, polarized, and completely resolved features are observed that can readily be identified with specific molecular units. An example includes the early Raman[1] work on nonstoichiometric Ge_xS_{1-x} glasses which *unambiguously revealed* molecular phase separation in this binary. Normal modes of S_8 rings were observed in Raman spectra of S-rich $(x<\frac{1}{3})$ alloys of this binary. It now appears that this phase separation is a general feature[1-3] of binary Y_xS_{1-x} glasses where $Y=$Ge, As, or Si. When vibrational bands overlap, as in the case of the Ge-rich alloys $(x>\frac{1}{3})$, the effectiveness of vibrational spectroscopy as a structure probe is largely impaired. Unambiguous analysis of the vibrational bands becomes difficult. The Raman spectrum of the stoichiometric glass $(g-)$ GeS_2 is a case in point. Two widely different structural interpretations of this spectrum have been advanced to date: one in which the network is regarded to be largely chemically ordered,[1,4] and the other in which broken chemical order[5] is an intrinsic feature of the glass network. In general, it appears that decoding such spectra becomes a major task. The task involves calculations of vibrational density of states in model network clusters rather than solely isolated building blocks of these clusters. This is the case because the observed density of states apparently contains vibrational modes characteristic of large clusters, i.e., medium-range order of the network. Choosing the appropriate clusters in these calculations can be the source of additional complications, particularly if the glass network contains structural elements that are peculiar to it, i.e., not found in corresponding crystals. Furthermore, because Raman scattering cross sections can easily vary by an order of magnitude from mode to mode, the observed mode scattering strengths do not necessarily reflect bond statistics of the network.

For these reasons, a completely independent source of information of a fully complementary nature can be invaluable in establishing structural models of glasses. Mössbauer spectroscopy[6] is ideal for this purpose as it can be used to probe site populations which are complementary to bond populations.

In this work we have examined bulk glasses of the composition $(Ge_{0.99}Sn_{0.01})_xS_{1-x}$ as a function of cation concentration x, using both Raman and Mössbauer spectroscopy (Secs. II and III). The central motivation of the present work is to reexamine the network structure of g-GeS_2, particularly its evolution from $x>\frac{1}{3}$ and $x<\frac{1}{3}$ in the light of new Mössbauer results. Our Raman spectra are in good agreement with the spectra of Ge_xS_{1-x} glasses reported earlier by a number of different groups. ^{119}Sn Mössbauer spectra are reported here for the first time. At the low Sn concentrations used in the present ternary glasses there is substantial evidence[6] to suggest that Sn atoms randomly replace the chemically inequivalent Ge sites of the network and serve as effective cation probes. The present Mössbauer results decisively favor a structural model of g-GeS_2 based on the principle of broken chemical order as was found earlier[7] for g-

$GeSe_2$. New clues in understanding the Raman vibrational spectra of these glasses have now been provided by the Mössbauer results. Specifically, the 250-cm^{-1} vibrational band that appears in the Ge-rich ($x > \frac{1}{3}$) glasses, which we propose in this work, is better understood as a mode of a GeS microphase rather than a normal mode of an ethane like unit.[8] This identification is strongly suggested by a correlation of the 250-cm^{-1} vibrational band strength with Mössbauer C site intensity. Both these spectroscopic features are found to vary linearly as a function of glass composition when $x > \frac{1}{3}$. Furthermore, because of an accidental overlap of Raman mode frequencies characteristic of $Ge(S_{1/2})_4$ units and $Ge_2(S_{1/2})_6$ units, molecular phase separation in g-GeS_2 has been difficult to recognize in vibrational spectroscopy. Specifically, the 340-cm^{-1} band, in g-GeS_2 usually identified as the symmetric stretch of $Ge(S_{1/2})_4$ units, is better understood as having scattering contributions from both the A_1 mode of $Ge(S_{1/2})_4$ units and the A_1g mode of $Ge_2(S_{1/2})_6$ units. It then becomes feasible to understand why the scattering strength of the 340-cm^{-1} band does not vanish even when x exceeds 0.40, a composition beyond which tetrahedral $Ge(S_{1/2})_4$ units are not expected to be present in the Ge-rich glasses.

Our spectroscopic results show that there are similarities as well as contrasting differences between the network structure of g-GeS_2 and g-$GeSe_2$. For example, although both these stoichiometric glasses are phase separated on a molecular scale, the physical size of the clusters in the S-containing glass is, in general, smaller (by factor of 2 or more) than in the Se-containing glass.[6,7] In the S-rich ($x < \frac{1}{3}$) glasses, small S-rich clusters such as S_8 monomers are prevalent, in corresponding Se-rich ($x < \frac{1}{3}$) glasses, extended Se-rich polymeric chains occur. In the Ge-rich alloys ($x > \frac{1}{3}$), rocksalt-like octahedral GeX structures (X=S and Se) readily appear. These appear when x exceeds 0.37 in the Se glasses, but appear already when x exceeds 0.33 in the S glasses. After presenting our experimental results in Sec. III, a discussion of structure of the stoichiometric glasses is given in Sec. IV. We conclude this paper with Sec. V where we summarize our principal findings.

II. EXPERIMENTAL CONSIDERATIONS

Ternary $(Ge_{0.99}Sn_{0.01})_xS_{1-x}$ glasses ($\frac{1}{2}$ g size) over a wide range of composition $0 \leq x \leq 0.43$ were prepared by alloying the pure elements in 5-mm-i.d. fused silica ampoules and quenching the melts in water. The melts were equilibrated at 800 °C up to 200 hours with periodic shaking after having held the melts at 950 °C (melting point of Ge) for 24 hours.

Raman scattering and Mössbauer spectra of the glasses were studied systematically as a function of glass composition. At the stoichiometric composition $x = \frac{1}{3}$, sample homogeneity was examined by recording spectra of different segments of the as-quenched melt (virgin glass). Furthermore, Mössbauer spectra of the virgin GeS_2 glass were also taken as a function of thermal annealing both below and above T_g to elucidate thermally induced structural effects.

The glass transitions of the samples were studied using a model 2C, differential scanning calorimeter from Perkin-Elmer. The scanning rate for these measurements was 20 K/min, and the glass transition temperature T_g was defined in the usual way as the halfway point between the two temperatures where a change in slope occurs upon the endothermic excursion.

Room-temperature Raman spectra were taken with a Spex Ramalog 4-1401 (double monochrometer). Typical spectra were recorded using 20 mW of power at the sample with the 5145-Å line of an Ar-ion laser and 6-cm^{-1} resolution. Both powders and large sized pieces of the glasses were examined. In the bond-stretching regime, no differences were observed between the different forms of the glasses.

^{119}Sn Mössbauer spectra of the glasses were recorded at 4.2 K using a liquid-helium exchange gas Dewar. $^{119}Sn^m$ in $CaSnO_3$ was used as a source of the 23.8-keV gamma rays which were detected using a thin NaI scintillation counter. To suppress the contribution of the K_α and K_β x rays at 25.2 and 28 keV in the pulse height window, a thin Pd foil (100 mg/cm^2) was used. All spectra were analyzed using least-squares-fitting routines designed to run on an IBM-PC.[9]

III. RESULTS

A. Mössbauer spectroscopy

1. Composition dependence

Figures 1–3 summarize the principal Mössbauer results emerging from the present work. We find that although only one type of Sn site (site A) is seen in the S-rich ($x \lesssim \frac{1}{3}$) glasses, two sites (site A and B) occur at the stoichiometric composition $x = \frac{1}{3}$, while at least three distinct types of Sn sites (A, B, and C) are populated in the Ge-rich glasses ($x > \frac{1}{3}$). We define site A as the narrow single line centered near $v = 1$ mm/s and site B as the quadrupole doublet populated when x exceeds a threshold value of 0.32. This particular site is found to grow rapidly in intensity with x above this threshold value. In the Ge-rich alloys ($x > \frac{1}{3}$), deconvolution of the spectra in terms of two sites (site A and B) was found, in general, to yield systematic misfits in line intensities of the B-site doublet. This is suggestive of a third site present in these glasses, as can be seen from Fig. 3 where a spectrum of a glass sample at $x = 0.34$ is analyzed both in terms of two sites (A and B), as well as three sites (A, B, and C). The better quality of the fit with three sites is, of course, not unexpected; is the inclusion of a third site to deconvolute the spectra necessary? The glass composition evolution of the spectra display an intensity asymmetry of the doublet which increases with x, with the more intense member of this doublet also having the narrower linewidth. Such a line-shape evolution of the doublet cannot be explained in terms of one quadrupole doublet, i.e., B sites, alone. It requires the presence of a third site. Analysis of the spectra in terms of three sites at compositions $x > \frac{1}{3}$ not only provides significantly better quality of fits, but as we discuss later in Sec. IV, such a procedure provides a natural link to understand the Raman scattering results as well.

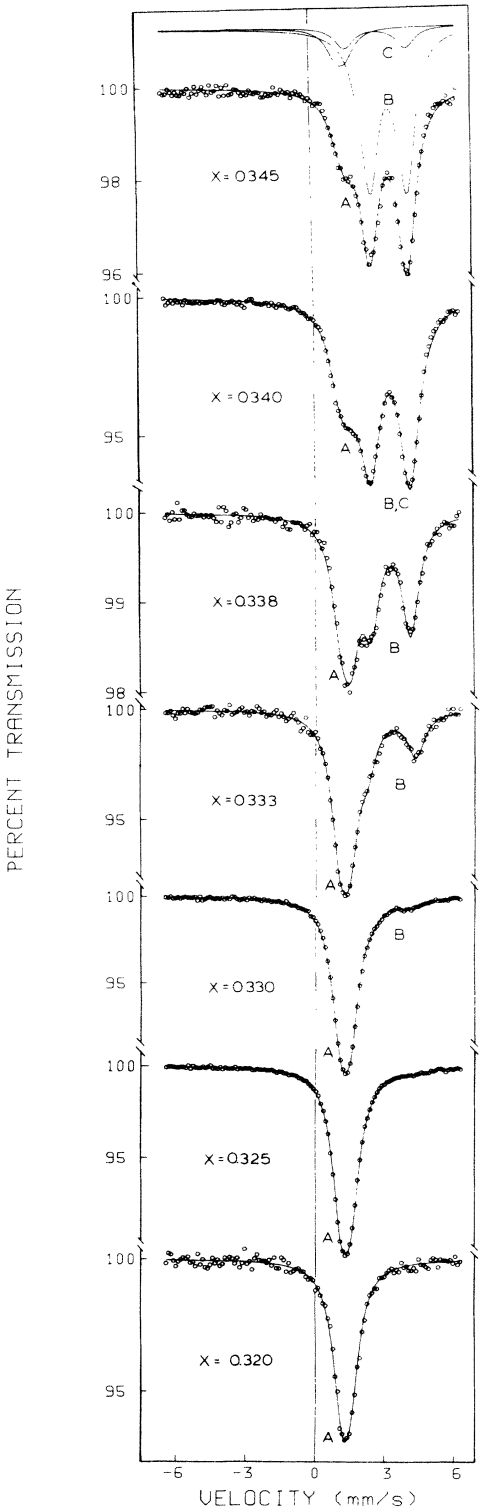

FIG. 1. Mössbauer spectra of $(Ge_{0.99}Sn_{0.01})_xS_{1-x}$ glasses taken as a function of cation concentration x. In the spectra, note that one site (A) is observed when $x < \frac{1}{3}$, but two sites (A and B) appear at $x = \frac{1}{3}$ and three sites (A, B, and C) appear when $x > \frac{1}{3}$.

The Mössbauer site intensity ratios for these glasses is displayed in Fig. 4 as a function of glass composition. For comparison purposes, results on corresponding Se-containing glasses taken from Ref. 10, are also reproduced in that figure. A comparison of these systematics reveals several noteworthy features: One finds that (a) two types

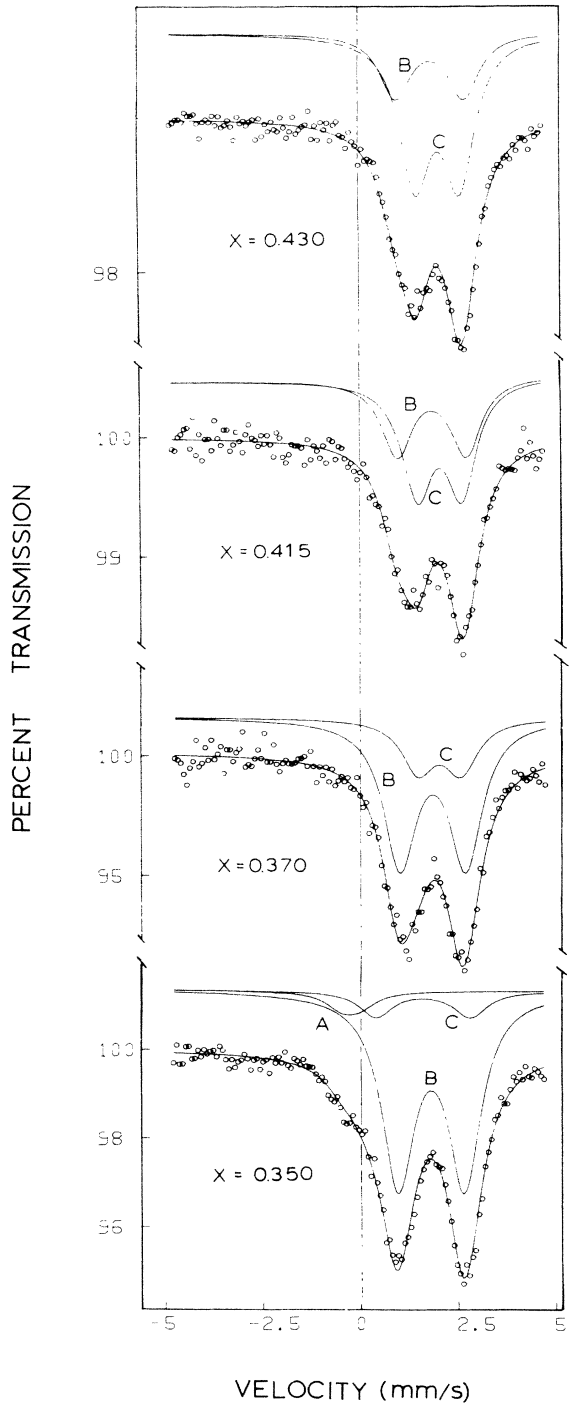

FIG. 2. Mössbauer spectra of $(Ge_{0.99}Sn_{0.01})_xS_{1-x}$ glasses for x in the range $0.35 \leq x \leq 0.43$. The smooth line through the data represents a least-squares fit to two quadrupole doublets for $x > 0.35$. Note that the A site is not observed for $x > 0.36$. See also Fig. 4.

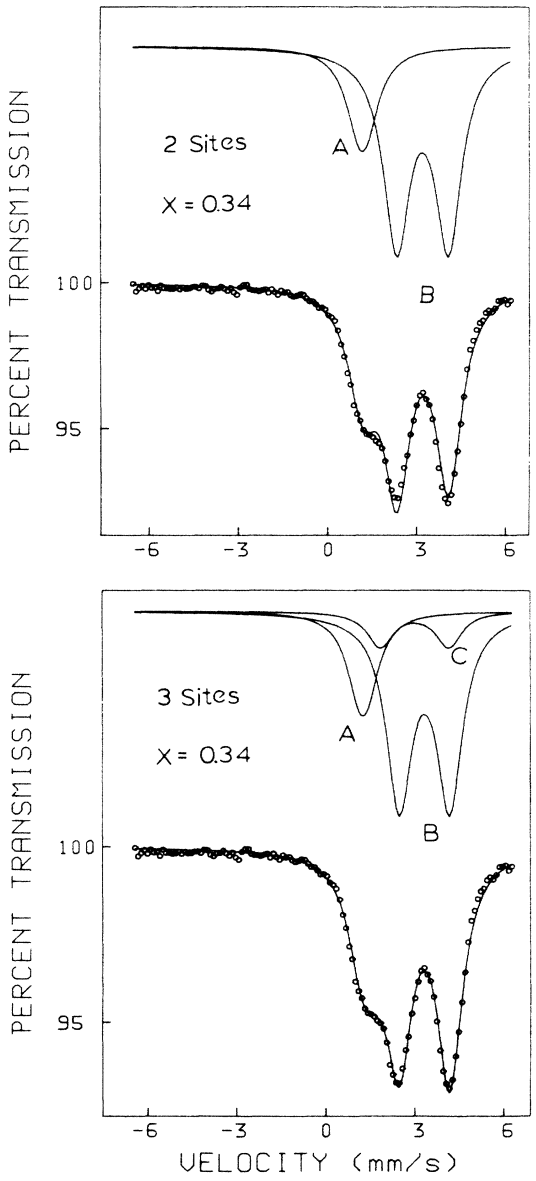

FIG. 3. A two- and three-site fit to spectrum of g-$(Ge_{0.99}Sn_{0.01})_{0.34}S_{0.66}$. Note that the intensity misfits appearing in the two-site fit disappear in the three-site fit.

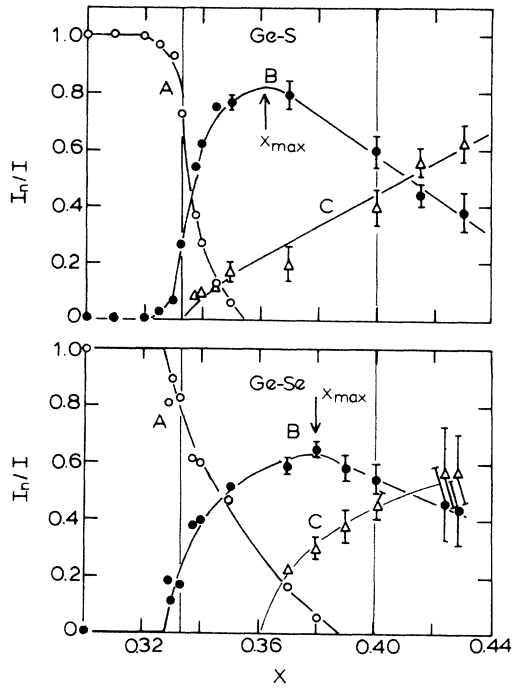

FIG. 4. Mössbauer site-intensity ratio I_n/I ($n=A$, B, and C) in g-$(Ge_{0.99}Sn_{0.01})_xS_{1-x}$ (top) and in g-$(Ge_{0.99}Sn_{0.01})_xSe_{1-x}$ (bottom) deduced from a deconvolution of the spectra. Note the presence of multiple sites (broken chemical order) at the stoichiometric compositions $x=\frac{1}{3}$ and $\frac{2}{5}$. The results on Se-containing glasses are taken from Ref. 10.

of sites (A and B) are populated, in general, at the stoichiometric composition $x=\frac{1}{3}$ with the site intensity ratio $I_B/I=0.29(2)$ for GeS_2 and 0.16(1) for $GeSe_2$ glass; (b) in the S glasses the site intensity ratio I_B/I, starting from a value of 0 at $x=0.32$, rapidly increases to acquire a value of 0.80(2) at $x=0.36$; (c) furthermore, I_c/I, starting from a value of 0 at $x=\frac{1}{3}$, continues to increase monotonically with x in the composition range $0.333 \leq x \leq 0.43$. These systematics will be correlated with Raman mode scattering strengths in Sec. III.

The nuclear hyperfine structure parameters of various sites deduced from a line-shape analysis of the spectra appear in Fig. 5. In principle, this data contains direct information on the microscopic nature of the various sites. In practice, a comprehensive interpretation of this data requires theoretical analysis of the electric field gradient (EFG) tensor and contact charge density $\psi(0)^2$ and this will be discussed elsewhere. We will, however, draw upon these experimental results to substantiate our claims on site identification using arguments based upon site symmetry.

2. *Sample homogeneity*

We present results of two additional experiments performed on g-GeS_2. Because the shape of the Mössbauer spectra were found to be unusually sensitive to the glass stochiometry near $x=\frac{1}{3}$, we were concerned with sample homogeneity. Raman and Mössbauer spectra of different segments of a virgin GeS_2 glass sample were examined. First, Raman spectra of the virgin glass in the silica ampoule were recorded at four different locations (A–D) along the length of the ampoule (Fig. 6). Next, samples from these locations were carefully removed and Mössbauer spectra of these samples taken. Figure 7 provides a summary of the spectra.

A cursive examination of the spectra shown in Figs. 6 and 7 reveals that the GeS_2 glass samples are, in general, quite homogeneous. Specifically, the Mössbauer site intensity ratio I_B/I as well as nuclear hyperfine structure parameters are found to be quite independent of sample

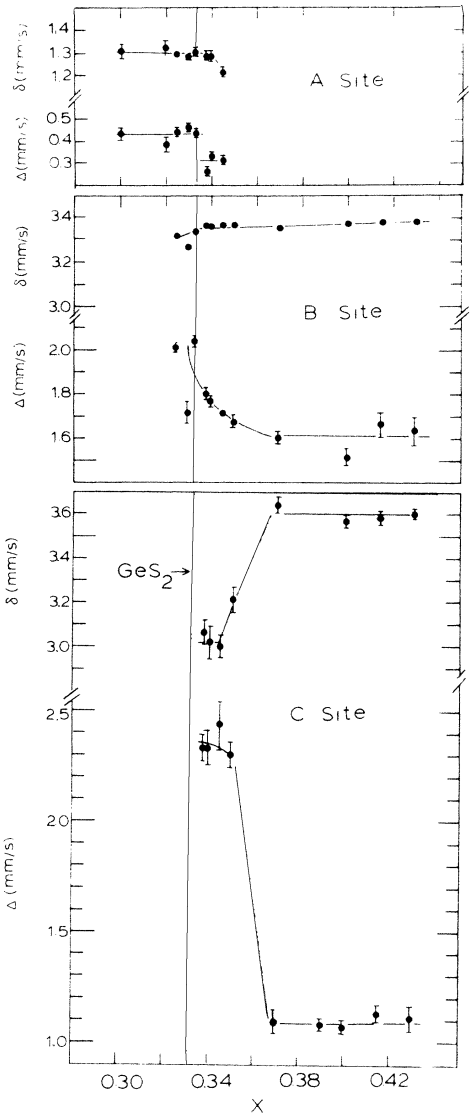

FIG. 5. x dependence of the isomer shift (δ) and the quadrupole splitting (Δ) of sites A, B and C.

location in the silica ampoule. Raman spectrum of the sample taken from location D is found to be slightly S rich however. In this case there is a hint of the S—S stretch mode (characteristic of S_8 rings of S^n chains) present at 486 cm^{-1}. Based on these results we would place an upper limit to sample inhomogeneity to be about 0.5 at.%. Raman spectra of samples taken along the length of the silica ampoule at locations A, B, and C also reveal very weak scattering at 486 cm^{-1} which appears *concomitantly* with an equally weak feature present at 250 cm^{-1}. The later feature is a signature of a GeS microphase as discussed later in Sec. IV C. We consider the appearance of both these weak features simultaneously as evidence for traces of disproportionation of g-GeS_2 by the reaction

$$GeS_2 = GeS + S \,. \tag{1}$$

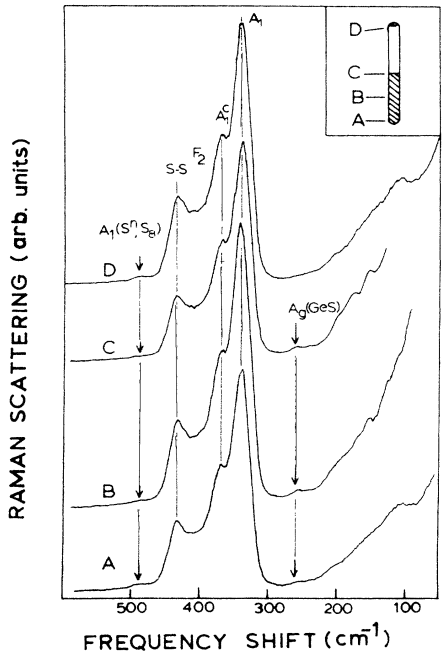

FIG. 6. Raman spectra of g-$Ge_{0.99}Sn_{0.01}S_2$ samples taken from locations A, B, C, and D along the length of the silica ampoule (see inset) used for melt quenching. See text for further details.

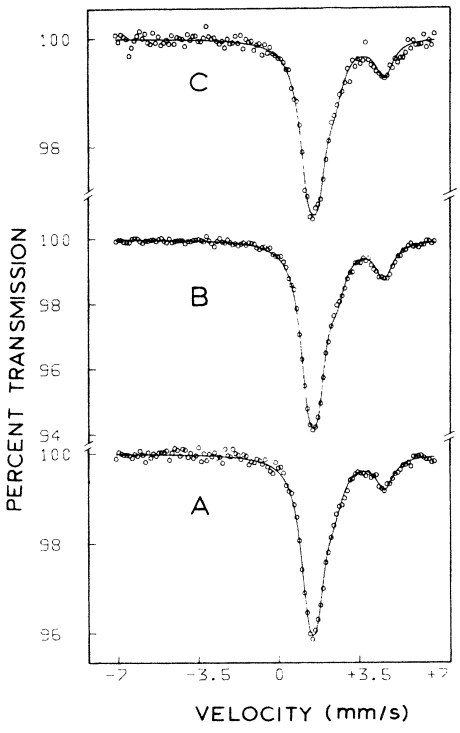

FIG. 7. Mössbauer spectra of g-$Ge_{0.99}Sn_{0.01}S_2$ samples taken from locations A, B, and C along the length of the silica ampoule. See inset of Fig. 6 for additional details.

3. *Thermal treatment and crystallization of GeS_2 glass*

Figure 8 provides Mössbauer spectra of g-GeS_2 taken as a function of heat treatment. Cycling the glass through $T=T_g$ for 15 min and also at $T=T_g+27$ °C for 15 min produced no measurable changes either in the site intensity ratio or line locations. However, upon heating the glass sample to 534 °C, i.e., 10 °C above the crystallization temperature, drastic changes in both the physical appearance of the sample as well as the shape of the spectrum were noticed. The sample color changed from yellow to darker yellow, almost brown. In the spectrum, a pronounced doublet having an isomer shift and quadrupole splitting characteristic of crystalline (c) SnS appeared while the doublet characteristic of site B of the glass completely disappeared. No detectable changes either in the width or the centroid of the site-A resonance could be detected. These heat-treatment effects have close parallels to those found[11] in g-$GeSe_2$ and are briefly understood as follows. Upon crystallization, some of the Sn dopant continues to remain tetrahedral (site A), this time present in the layered structure of c-GeS_2 replacing some of the Ge sites. The excess Sn, which apparently could not dissolve in the c-GeS_2 phase, segregates into Sn-rich clusters which consist of SnS crystallites.

B. Raman spectroscopy

Infrared reflectance and Raman spectra of g-GeS_2 have been reported by a number of previous workers.[1,4,8] These results, in general, are in good agreement with each other. Our Raman spectrum obtained for a sample at $x=\frac{1}{3}$ is also in good accord with these earlier reports and is shown in Fig. 6. The presence of Sn traces in our samples do not lead to discernable new features in the vibrational spectrum as expected.

There is general recognition that the 340-cm^{-1} feature represents the A_1 symmetric stretch of $Ge(S_{1/2})_4$ tetrahedral units. The 374-cm^{-1} feature, designated as the companion A_1^c mode, is generally associated with medium-range order, although the precise nature of the latter has been a matter of some controversy.[12] Density of vibrational states calculations[13] in specific molecular clusters favor the more recent interpretation of this mode as a cluster edge mode. These calculations[13] also show that the 440-cm^{-1} mode represents a S—S stretch coming from cluster edge dimers. The compositional variation of the vibrational spectra (shown in Fig. 9) reveals the following trends. (a) The 475-cm^{-1} mode that is present in the S-rich glasses ($x<\frac{1}{3}$) vanishes in the Ge-rich glasses ($x>\frac{1}{3}$). (b) The 250-cm^{-1} mode first emerges when $x>\frac{1}{3}$, and its scattering strength normalized to the 340-cm^{-1} mode increases nearly linearly in the composition range $0.333<x<0.360$ (Fig. 10). Finally, (c) the 340-cm^{-1} mode appears in the spectra over a very wide range of composition $0\leq x\leq 0.43$. These observations are quite similar to those reported earlier[1,4,14,15] by a number of previous workers.

C. Differential scanning calorimetry

Figure 11 summarizes the glass transitions (T_g) of the present glasses near the composition $x=\frac{1}{3}$. These results reveal a maximum of T_g at the stoichiometric composition[16] $x=\frac{1}{3}$, and this is related to a maximum in the number of heteropolar Ge—S bonds at this composition.

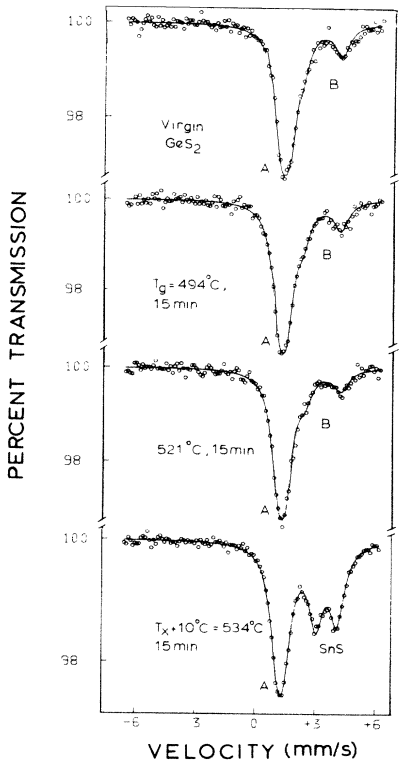

FIG. 8. Mössbauer spectra of g-$Ge_{0.99}Sn_{0.01}S_2$ samples subjected to indicated heat treatments.

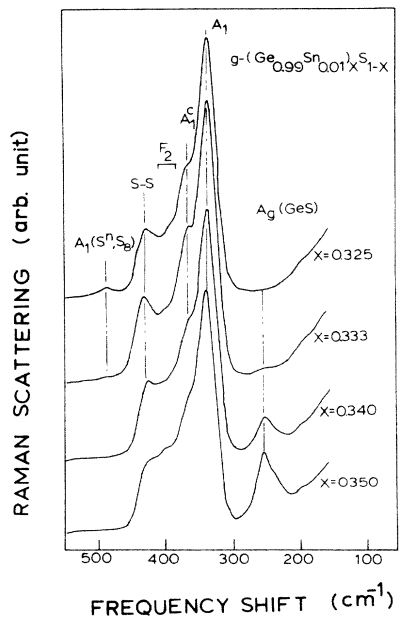

FIG. 9. Room-temperature Raman spectra of indicated glasses showing evolution of the 250-cm^{-1} mode in the Ge-rich ($x>\frac{1}{3}$) phase.

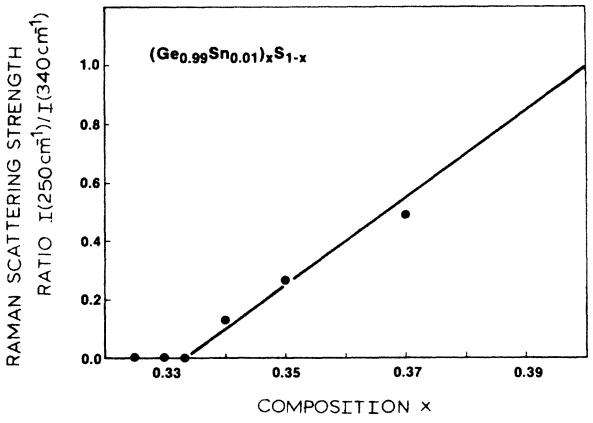

FIG. 10. Raman scattering strength ratio of the 250-cm^{-1} mode to 340-cm^{-1} mode as a function of glass composition x from the spectra of Fig. 9.

Both above and below $x=\frac{1}{3}$, the population of homopolar bonds Ge—Ge and S—S sharply increases and this presumably is related to the T_g reduction. The trend of a reduction in T_g in the Ge-rich glasses, which is more drastic than in the S-rich glasses, we suspect derives from a general lowering of the intercluster forces as a new more rigid cluster (C cluster) appears when $x > \frac{1}{3}$. We will return to this point later.

IV. DISCUSSION OF RESULTS

The broad physical picture of the GeS_2 glass network emerging from the present work may be stated. The atomic scale structure of the stoichiometric glass is visualized to be heterogeneous and specifically to consist of two types of molecular clusters as shown in Fig. 12: an A cluster possessing a quasi-two-dimensional structure and a

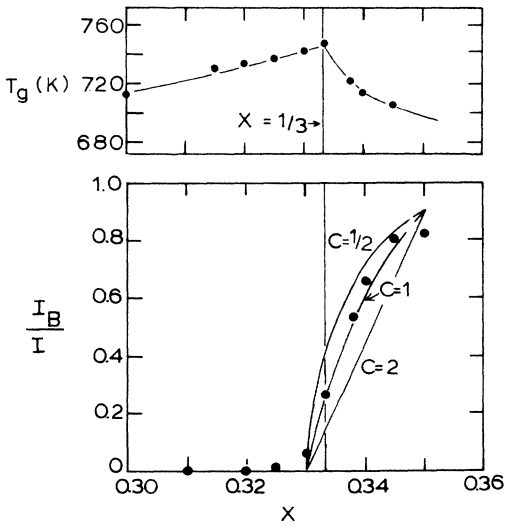

FIG. 11. Glass transition temperature T_g (top) and Mössbauer site-intensity ratio I_B/I (bottom) as a function of glass composition x. See text for further details.

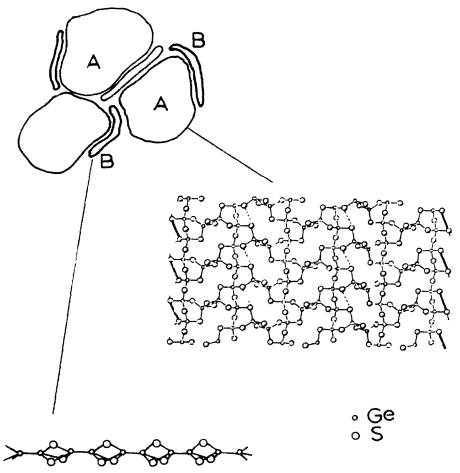

FIG. 12. Heterogeneous structure of GeS_2 glass consisting of large A and small B molecular clusters. The A cluster is thought to be a fragment of the high-temperature phase of c-GeS_2 which has been reconstructed to have S—S dimers at its edges. A cluster containing four corner-sharing chains is consistent with the observed broken cation chemical order in g-GeS_2. The B cluster is believed to be a fragment of a quasi-one-dimensional ethanelike chain having $Ge_2(S_{1/2})_6$ building blocks.

B cluster consisting of quasi-one-dimensional chains. The intracluster interactions are primarily covalent while the intercluster ones are largely van der Waals in character.

The mass density deficit in a glass in relation to its crystal is thought to arise from the intercluster volume. At and above the softening temperature $T=T_g$ of a glass network, the weaker intercluster interactions are overwhelmed although the intracluster interactions (molecular clusters) are largely held intact as suggested by the high viscosities of glass-forming (polymeric) liquids. In this section we will show how the present Mössbauer and previous Raman and diffraction results refine in a coherent fashion the broad physical picture of molecular clusters described above.

A. Mössbauer sites, glass molecular clusters, and glass-forming tendency

Profound similarities and contrasting differences appear in Mössbauer site intensity ratios [$I_n/I(x)$ where $n=A$, B, and C] between the present S-containing glasses and the corresponding Se-containing glasses as shown in Fig. 4. In both systems we find close parallels in site signatures and site intensity ratios as a function of glass composition. The microscopic origin of these sites was discussed in detail for the Se-containing glasses elsewhere. The site identification developed in Ref. 10 applies equally well for the present S glasses. Briefly, these sites represent Sn replacing Ge sites in three distinct molecular clusters. Site A: a quasi-two-dimensional layered structure of GeS_2 nominal stochiometry, whose morphology is similar to the high-temperature phase of c-GeS_2. In this molecular phase all cations are tetrahedrally coordinated.

Site *B*: a quasi-one-dimensional chainlike cluster whose building block consists of an ethanelike $Ge_2(S_{1/2})_6$ unit. The doublet nature of this site arises due to broken tetrahedral symmetry when Sn replaces one of the Ge sites in such a unit; in such a unit Sn is present in a local trigonal symmetry. Site *C*: a quasi-two-dimensional layered structure based on *c*-GeS. In this distorted rocksalt structure the Sn for Ge replacement leads to Sn^{2+}, which is locally coordinated to three short and three long S near neighbors.

The site intensity ratios of Fig. 4 clearly serve to demonstrate that the *C* microphase appears only when $x > 0.37$ in the Se-containing glasses, but already appears when $x > 0.33$ in the S-containing glasses. This radical difference in behavior between the two chalcogenide glasses can be traced to the higher Pauling electronegativity[17] of S(2.5) in relation to Se(2.4) which promotes formation of ionic structures, such as the *C* microphase. In both cases the site intensity ratio I_c/I is found to monotonically grow with x in the range $0.33 < x < 0.42$. From Fig. 4, we find that once x exceeds 0.42, $I_c/I > 0.5$, i.e., the *C* microphase becomes the majority phase. It is well known[16] that bulk glass formation ceases when the cation concentration exceeds 0.42 in both these binary glasses. This behavior can be understood in terms of the more rigid or overconstrained character[18] of the *C* microphase which is not conducive to forming elastic networks. In the *A* and *B* microphases both the cations and anions conform to the 8-*N* coordination rule. The reverse is true for the *C* microphase in which the pronounced rigidity, we believe, derives from the bonding electrons being partially transferred (ionic) rather than being shared (covalent) between the atoms. The molecular cluster model[19] provides a natural microscopic explanation for the glass-forming tendency.

B. Molecular cluster size in GeS_2 glass

The Mössbauer site-intensity-ratio results of Fig. 4 show that at $x = \frac{1}{3}$, $I_B/I = 0.29(2)$ in the S-containing glasses. In the corresponding Se-containing glasses this ratio was found to be substantially smaller at 0.16(1). The structural significance of this observation[7] is that the size of the *A* microphase in GeS_2 glass is substantially smaller than the corresponding size in $GeSe_2$ glass.

In the composition range $0.32 < x < 0.35$, one observes predominately *A* and *B* sites while the population of *C* sites remains $I_c/I < 0.10$. To a good approximation glass networks near the composition $x = \frac{1}{3}$ can therefore be described in terms of two microphases only. To arrive at the degree of broken chemical order, i.e., the fraction of ethanelike Ge sites in *g*-GeS_2, one has to establish the Sn-site preference energy $(E_A - E_B)$. Following the two-site theoretical model developed in Ref. 7, the site intensity ratio I_B/I can be written as

$$I_B/I = N_B/(CN_A/2 + N_B) = \frac{x - x_0}{C(x_1 - x)/2 + (x - x_0)} , \quad (2)$$

where N_A and N_B represent population of *A* and *B* sites of the network,

$$C = \exp[(E_B - E_A)/k_B T_g] ,$$

and the end member compositions x_0 and x_1 are defined by $I_B/I\ (x = x_0 = 0.328) = 0$, $I_B/I (x = x_1 = 0.35) = 0.90$. In Fig. 11 we plot Eq. (2) for different *C* values and find that $C = 1$ is a reasonably good fit to the observed site intensity ratio. This indicates that the site preference energy $E_A - E_B = 0$, i.e., $E_B = E_A$. Under the circumstance, it can be shown from Eq. (2) that $I_B/I = N_B/N$. The fraction of nontetrahedral Ge sites in GeS_2 glass is thus deduced to be 0.29(2).

It would be important to recall here that the trend of a rapid growth in I_B/I near $x = \frac{1}{3}$ is incompatible with the notion that *B* sites represent isolated bonding defects (Ge—Ge homopolar bonds) in the *A* microphase. As discussed earlier,[7] the maximum growth rate of homopolar Ge—Ge bonds as a function of glass composition x, i.e., the slope $d/dx(N_{\text{Ge-Ge}}/N)$ equals a value of 18 in a chemically ordered continuous random network model. This is to be compared to the value of $d/dx(I_B/I) = 61(4)$ deduced from the results of Fig. 11. The reader is referred to Ref. 7 for a detailed discussion of this point.

In *g*-GeS_2, the presence of a finite number of Ge—Ge bonds deduced from the present experiments, on grounds of stochiometry, requires that there be an equivalent number of S—S bonds. Evidence[20] for such bonds has been obtained indirectly from Mössbauer EFG measurements using a chalcogen atom ($^{129}Te^m$). In these experiments two distinct and chemically inequivalent ^{129}I sites are observed. These sites originate because the radioactive $^{129}Te^m$ atoms alloyed in *g*-GeS_2 can either replace S sites that are twofold coordinated to Ge, i.e., the chemically ordered sites, or replace S sites that have one Ge and one S near neighbor, i.e., the chemically disordered sites. Because these $^{129}Te^m$ sites upon nuclear transmutation yield a onefold coordinated daughter ^{129}I atoms that can either be bonded to Ge near neighbor or to a S near neighbor, drastically different EFG's result and permit discriminating between the two types of sites. Apparently because the Te site preference energy for the chemically disordered site is substantially higher than for the chemically ordered sites, the Te occupied site population ratio of disordered to ordered sites of 1.60(5) is found[20] to be an order of magnitude larger than the actual ratio (0.3) of disordered to ordered sites. The details of these experiments and analysis are discussed elsewhere.[20]

One may arrive at the *A* cluster size from the deduced degree of broken chemical order $I_B/I = 0.29(2)$ (in the present ^{119}Sn experiments) by describing phase separation of molecular clusters as follows:

$$\tfrac{102}{5}GeS_2 = \tfrac{2}{5}Ge_{16}S_{27}\ (B \text{ cluster}) + Ge_{14}S_{30}\ (A \text{ cluster}) . \quad (3)$$

In writing the above equation we have assumed that the stoichiometry of the *B* cluster is approximately given by $Ge_{0.36}S_{0.64}$, corresponding to a maximum in I_B/I. Since each Ge site in the *A* (*B*) cluster is tetrahedral (nontetrahedral), the fraction of nontetrahedral Ge sites implied by Eq. (3) becomes

$$I_B/I = 6.4/20.4 = 0.31 \quad (4)$$

in reasonable accord with the experimentally deduced value of 0.29(2).

One possible interpretation of the stoichiometry of the A cluster is that it implies an "outrigger raft" having a lateral width[6] of about 30 Å corresponding to four corner sharing chains of $Ge(S_{1/2})_4$ units. The outrigger raft represents a molecular fragment of the layered crystalline form of GeS_2 (β-GeS_2) whose edges have been reconstructed to have S—S bonds. This cluster, first suggested by Bridenbaugh *et al.*[5] in connection with Raman scattering of g-$GeSe_2$, is thought of as the acceptor cluster of these phase-separated glasses. The molecular cluster size in g-$GeSe_2$ is found[6,7] to be twice as wide as the one deduced here for g-GeS_2. In general, it appears that Se-containing glasses are better polymerized than their S counterparts, a fact which may intrinsically be the consequence of a higher bonding strength[17] of S—S bonds in relation to Se—Se bonds.

The mass density of β- and g-GeS_2 have been measured and are found to be 2.88 g/cm^3 (Ref. 16) and 2.717(6) g/cm^3 (Ref. 16), respectively. The molar volume surplus in GeS_2 glass implied by this data is 5.7%. In β- and g-$GeSe_2$ the densities are established to be 4.39 g/cm^3 (Ref. 21) and 4.229(24) g/cm^3 (Ref. 22), indicating a molar volume surplus of only 3.7%, i.e., nearly half as much. These macroscopic results qualitatively reinforce the present findings from microscopic probes of glasses. The smaller physical size of molecular clusters in the S-containing glasses implies a larger interfacial volume, and it essentially accounts for the larger molar volume surplus in g-GeS_2 in relation to g-$GeSe_2$.

C. Structural origin of 250-cm^{-1} Raman vibrational mode in Ge_xS_{1-x} glasses

The strong correlation of the Mössbauer C-site intensity ratio I_c/I with the 250-cm^{-1} Raman mode scattering strength, both studied as a function of glass composition, suggests that these spectroscopic features are signatures of the same structural unit. In this section we discuss the origin of this mode. Specifically, we show that it represents the breathing mode of double layers characterizing the structure of distorted rocksalt GeS microphase.

Our approach is to first examine optical phonons of c-GeS and identify the strongest Raman active mode. Next our working hypothesis is that the strongest Raman-active mode in the crystal is also the strongest Raman-active mode in the corresponding glass. Experience on tetrahedral glasses has indeed shown this to be the case. The optic modes in molecular glasses can somewhat shift and usually broaden in relation to those in the crystals, although their microscopic character and scattering strength remains largely intact.

Raman scattering and infrared reflectance of the IV-VI semiconductors GeS, GeSe, SnS, and SnSe, which crystallize in a distorted rocksalt structure (Fig. 13), have been extensively investigated.[23–25] To understand the optical phonons in these materials, one has to recognize that there are two relevant crystal symmetries: the D_{2h}^{16} space-group symmetry of the three-dimensional crystal and a diperiodic symmetry (DG32) of an individual double layer. There exists a center of inversion between the double layers but

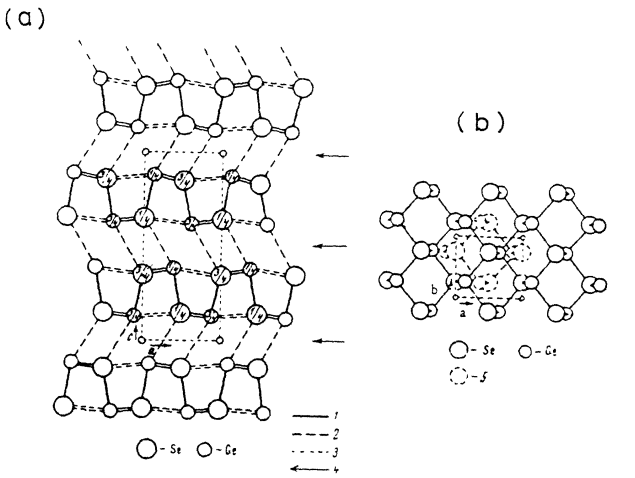

FIG. 13. The distorted rocksalt structure of c-GeSe showing presence of double layers running along the c axis. The figure is taken from Abrikosov *et al.*, Ref. 21.

no such symmetry operation in a given double layer. This has the important consequence that if the interlayer coupling is weak in relation to the intralayer forces, then the Raman and infrared (ir) active phonons are degenerate. Switching on the interlayer coupling leads to a lifting of the mode degeneracy as a Davidov splitting emerges. Such splittings have served[26] as important optical probes of the layered or two-dimensional (2-D) character of these semiconductors.

It is well known that the most intense optic mode corresponds to the diagonal matrix elements of the Raman tensor corresponding to Ag modes. For the D_{2h}^{16} space group, a group-theoretical analysis[23,24] of the zone center optical phonons predict 4-A_g modes. The experiments do indeed confirm this theoretical prediction. In c-GeS the four modes in question occur at 48, 111, 238, and 269 cm^{-1}. The lowest-frequency mode (48 cm^{-1}) represents a rigid-layer mode in which one of the double layers as a rigid unit moves against another double layer. The highest-frequency mode (269 cm^{-1}) is a rocksalt mode in which the anion sublattice beats against the cation sublattice. This is the reststrahlen mode which is expected to be strongly infrared active, as is confirmed by experimental results shown in Fig. 14 of Ref. 23. The second-highest optic mode (238 cm^{-1}) and third-highest optic mode (111 cm^{-1}) are modes characteristic of the double layers. These intradouble layer modes have been respectively identified[24] as layer-breathing (238 cm^{-1}) and layer-waving (111 cm^{-1}) modes. In this context it is important to note that while the 111-cm^{-1} mode is ir active, the 238-cm^{-1} mode is not. This is seen in Fig. 14, lower box depicting ir reflectivity for the E||a axis which shows a feature at 118 cm^{-1} but not one near 238 cm^{-1}. This is more clearly depicted in Table III of Ref. 23, which identifies the Raman-infrared Davidov doublets ($A_g - B_{1u}$). Note that the infrared B_{1u} companion of the Raman-active A_g mode at 238 cm^{-1} is missing. Surprisingly this is the *only* missing phonon in the family of the IV-VI semiconductors.

In *c*-GeSe, the 4-A_g modes are observed[24] in Raman scattering at 39, 83, 174, 182 cm^{-1} (Fig. 15). Kramers-Kronig analysis of the optical reflectance, as expected, reveals[24] ir activity corresponding to the 83-, 174-, and 182-cm^{-1} optic phonons. Note in Fig. 15, lower box, the infrared reflectance corresponding to $\mathbf{E}||\mathbf{a}$ exhibit B_{1u} phonons at 186, 175, and 88 cm^{-1}. This can be more clearly seen from Table 3 of Ref. 24. This pattern is also seen for *c*-SnS and *c*-SnSe, and the reader is referred to Ref. 25 for a complete discussion of the experimental results.

In *c*-GeSe and *c*-SnSe, the highest-frequency A_g modes are also found to possess a high Raman scattering cross section in general. In the corresponding sulfides, however, this is found not to be the case (see Figs. 14 and 15). Specifically, results on both *c*-GeS and *c*-SnS show that it is the second-highest-frequency A_g mode that exhibits an order of magnitude higher scattering strength than the highest-frequency A_g mode.

Raman signature of the GeS microphase in glasses must therefore consist of a mode that is the analog of the 238-cm^{-1} A_g mode and not the 269-cm^{-1} A_g mode seen in *c*-GeS. Specifically, we propose that the 250-cm^{-1} mode is a double-layer breathing mode of GeS microphase and has a character that resembles that of the 238-cm^{-1} A_g mode of *c*-GeS. In this context, the lack of ir activity of the 250 cm^{-1} is quite compatible with the lack of ir activity of the 238-cm^{-1} mode of *c*-GeS. This spectroscopic feature constitutes strong support for the proposed identification. Indeed previous contentions[27] against identifying the 250-cm^{-1} mode with a GeS microphase has been the lack of ir activity of this mode. Such contentions are based on the assumption that the 250-cm^{-1} mode is the analog of the highest-frequency restrahlen mode at 269 cm^{-1}.

Normally one expects a red shift of vibrational modes in going from a crystal to its less densely packed counterpart, the glass, such as seen for A_1 symmetric stretch of $Ge(Se_{1/2})_4$ units from 210 cm^{-1} in β-$GeSe_2$ to 202 cm^{-1} in *g*-$GeSe_2$. In a glass which evolves continuously from its liquid melt, one has a network structure that is effectively frozen at a negative pressure in relation to its crystalline structure. One may understand a red shift of modes in a glass with respect to the crystal in much the same way one understands a pressure-induced blue shift of modes in a molecular solid in an actual laboratory experiment.

Our identification of the 250-cm^{-1} A_g mode in the glass, as the analog of the 238-cm^{-1} A_g mode of *c*-GeS runs contrary to normal expectations and this deserves an explanation. The underlying anomaly can be traced to the distorted rocksalt structure of *c*-GeS which gives rise to bimolecular layers (Fig. 13). In this unusual structure, the interbimolecular interactions which involve van der Waals forces mediated by lone pairs, are distinctly weaker than the intrabimolecular interactions which are pronouncedly covalent in character. Understandably, the cleavage plane in *c*-GeS lies along the *b* axis (Fig. 13). In the *C* microphase of the glasses the integrity of the bimolecular layers may actually be enhanced at the expense of some loss in correlation between the bimolecular layers. We are suggesting that a partial transfer of strength occurs from interbimolecular to intrabimolecular interactions in the glass.

Such a conclusion is independently suggested by the Mössbauer quadrupole splitting parameters of the *C* site shown in Fig. 5. We draw attention to the steplike change in the Mössbauer *C*-site parameters near the composition

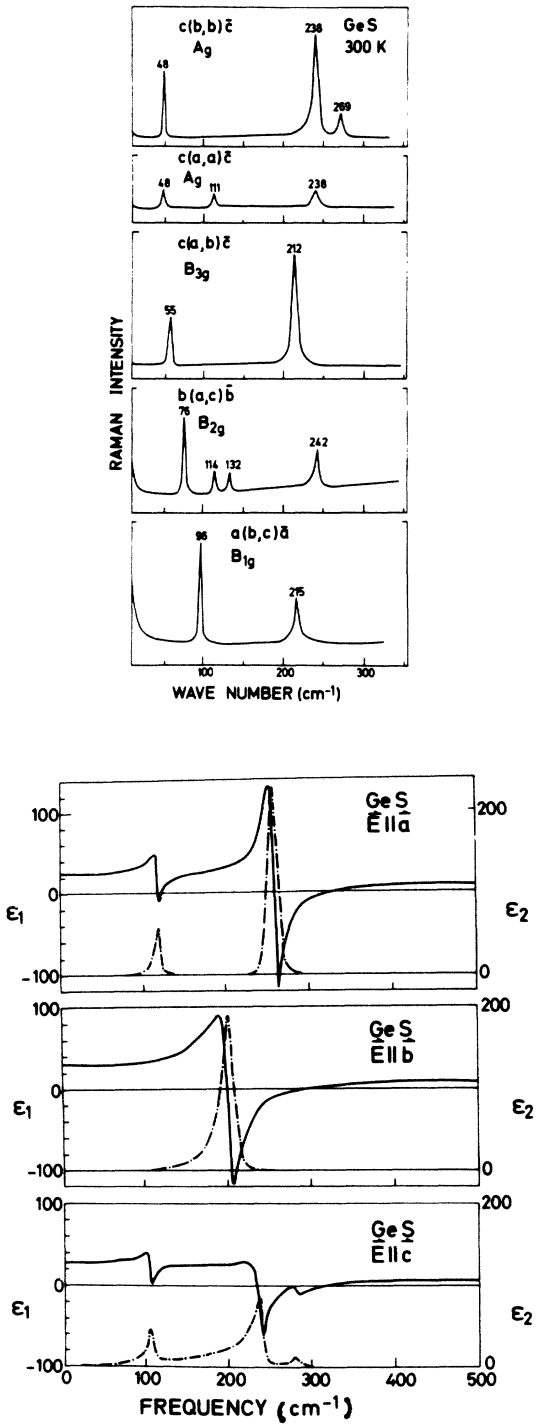

FIG. 14. Raman scattering and infrared reflectance of *c*-GeS taken from the work of Wiley *et al.* (Ref. 23), showing the 4-A_g mode. Note that the ir-active optic phonon corresponding to the Raman-active 238-cm^{-1} (double-layer breathing) mode is missing.

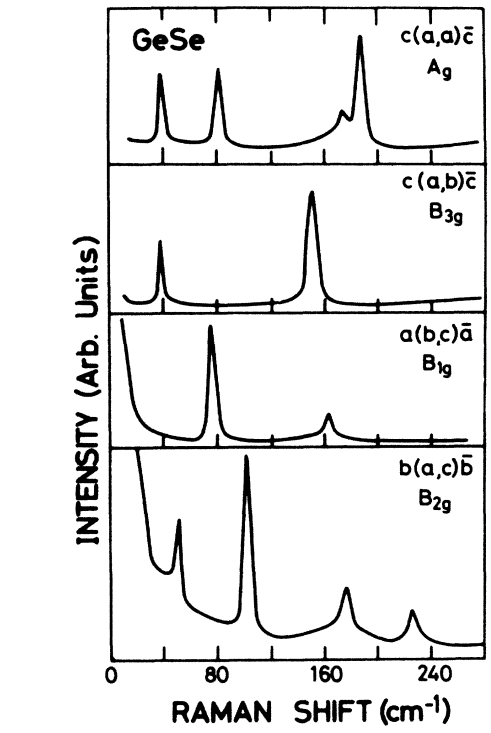

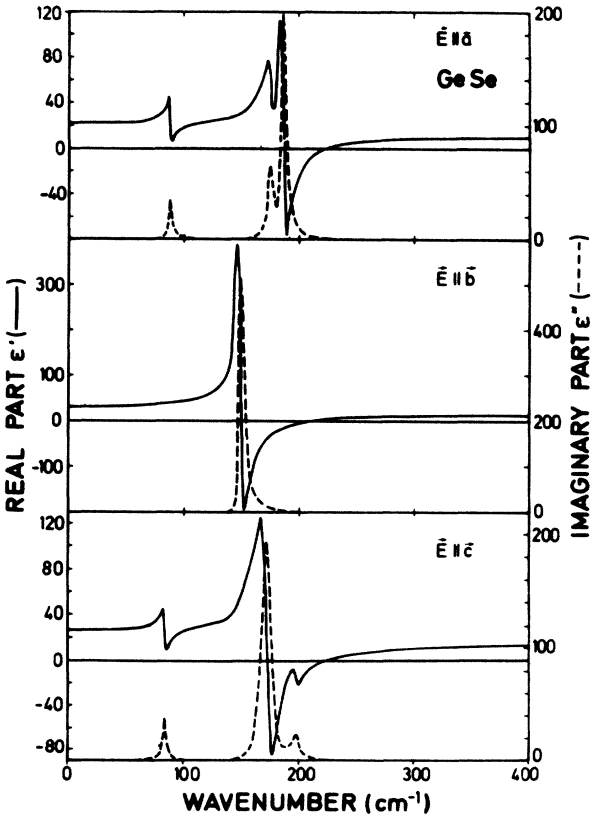

FIG. 15. Raman scattering and infrared reflectance of *c*-GeSe taken from the work of Chandrasekhar *et al.* (Ref. 24), showing the 4-A_g mode predicted by group theory. In this case note that the three A_g modes at 83, 174, and 182 cm^{-1} are all ir active.

$x = 0.36$. The origin of the step in Δ_c in Fig. 5 most likely derives from a change in dimensionality of the *C* clusters from 2D at $x < 0.36$ to 3D at $x > 0.36$. The quadrupole splitting is a direct measure of the cation local symmetry, particularly its symmetry departure from cubic character. The quadrupole splitting of 1 mm/s observed at $x > 0.36$ is characteristic of a Sn impurity atom replacing Ge sites in distorted rocksalt structure of *c*-GeS.

In summary, the origin of the blue shift in the bimolecular breathing mode is thus traced to an enhanced 2D character of the double layers in the glass. Crystallization of the *C* microphase is probably driven and stabilized by long-range ionic interactions which restore at least partially the 3D character at low temperature ($T < 580$ °C) and almost completely at higher temperature ($T > 580$ °C) where a transition to a cubic rocksalt phase has been suspected.[21]

D. The 340-cm^{-1} Raman vibrational band in Ge-S glasses and broken chemical order

The broader issue raised by the present Mössbauer results is how does one reconcile the molecular cluster model with the Raman spectrum of *g*-GeS_2. Specifically, what are the consequences of broken-site chemical order deduced from Mössbauer spectroscopy. In this section we address the underlying issue and show that there is a genuine difficulty in deducing the degree of broken-*bond* chemical order from Raman scattering because the ordered (Ge—S) and disordered (Ge—Ge) bonds of the network yield vibrational mode frequencies that are accidentally degenerate.

In the S-rich glasses there is overwhelming evidence that the scattering strength of the 340-cm^{-1} band increases nearly linearly with Ge content x. This result along with the strong polarization of this band constitutes strong evidence that in the S-rich glasses, the 340-cm^{-1} band represents the A_1 symmetric stretch of $Ge(S_{1/2})_4$ tetrahedral units, i.e., the chemically ordered Ge—S bonds.

There are several other observations concerning this band that suggest that while the above identification is necessary, it is not sufficient. Specifically, in the Ge-rich glasses, Raman scattering results[8,14] show that this band continues to be present at a high scattering strength even when $x = 0.40$. In fact, the band in question is observed for cation concentrations all they way up to $x = 0.43$, a composition which represents the limit of bulk glass formation[16] in this system. Indeed one would scarcely expect $Ge(S_{1/2})_4$ tetrahedral units to be present at any significant level in these glasses once $x > 0.40$.

The resolution of this spectroscopic anomaly rests in the general recognition that in the Ge-rich glasses and also for *g*-GeS_2 the 340-cm^{-1} band has contributions that arise *both* from A_1 modes of $Ge(S_{1/2})_4$ tetrahedral units *as well as* A_{1g} modes of ethanelike $Ge_2(S_{1/2})_6$ units. The calculations of Lucovsky *et al.*[8] actually reveal a Raman-active mode of ethanelike units to occur at 340 cm^{-1}. The mode in question is the higher-frequency mode of the two possible Raman-active normal modes of ethanelike units. The other mode frequency is estimated at 250

cm^{-1} by these calculations. The eigenvectors of the high-frequency mode consist of an out-of-phase motion of the S triad pair in relation to the Ge pair. Since this mode is symmetric in character, it is expected to be strongly polarized as confirmed by experiments.[8] Consequently, it is not possible to discriminate chemically ordered Ge—S bonds from chemically disordered Ge—Ge bonds in Raman scattering. Experimentally the situation in g-GeS_2 is additionally compounded by the fact that the width of the A_1 band (15 cm^{-1}) is nearly twice the width of the corresponding band in g-$GeSe_2$. This effect is due to some interfacial strain that is induced by the smallness of molecular cluster size in S glasses. Cryobaric Raman experiments of Weinstein *et al.*[28] have convincingly demonstrated that this large width is actually the result of a small internal pressure of <2 kbar between the molecular clusters.

Our proposal to use the 340-cm^{-1} mode (high frequency) rather than the 250-cm^{-1} mode (low frequency) as a bench mark of Ge_2S_6 ethanelike unit deserves a comment. Apparently in corresponding Ge_2Se_6 units, experiments suggest that it is the low-frequency Raman active mode at 180 cm^{-1} and not the high-frequency mode at 240 cm^{-1} that has the larger scattering cross section. Such a reversal in mode scattering cross sections from Se-containing to the S-containing molecular units, apparently is not peculiar to the B molecular phase. As discussed in Sec. IV C, such a behavior actually occurs for the C molecular phase as well. Predicting absolute cross sections of vibrational modes in Raman scattering is, in general, a nontrivial task even in crystals. It is at this time less clear to us what factors are specifically responsible for the reversal in mode scattering cross sections as a function of chalcogen type. Some of the factors that may account for such a behavior, in our view, must include (a) the electronegativity difference between S (2.5) and Se (2.4) that augments bond polarizabilities, (b) the actual geometry of the ethanelike unit (staggered versus eclipsed), and (c) the connectivity of the ethanelike units with the C and possibly A molecular phases of the glass network. This issue needs to be explored in the future.

Weinstein *et al.*[28] have noted the lack of complete reversibility in cryobaric Raman scattering experiments on g-GeS_2. Specifically, in these experiments one found that after release of high pressure, two new features appear in Raman scattering at 486 and 250 cm^{-1} which were originally absent in the spectrum of the virgin sample (taken at ambient pressure). The natural explanation of these vibrational features is that there is a pressure-induced densification of the A molecular phase in which a small segment of this phase has been irreversibly compacted by the disproportion reaction of Eq. (1). The appearance of 486- and 250-cm^{-1} modes after high-pressure cycling of the virgin glass are signatures of the S-rich (S_8 or S^n chains) and Ge-rich (GeS microphase) phases formed. The compacting is realized by the increased cation coordination from four in the A phase to six in the C phase. These results provide additional support for our identification of the 250-cm^{-1} mode with the C molecular phase.

It would be appropriate to recall here that in g-$GeSe_2$ the situation is more clearly understood. This is largely the case because the ordered (Ge—Se) and disordered (Ge—Ge) bonds give vibrational features at 202 and 180 cm^{-1}, i.e., resolved from each other. In this case the degree of broken-bond chemical order of 2% deduced from Raman bond spectroscopy is found to be completely compatible[6] with the measured 16% broken-site chemical order from Mössbauer spectroscopy. In experiments[29] on pseudobinary $(GeSe_2)_{1-x}(SnSe_2)_x$ glasses one has furthermore found that the scattering strength of the A_1^c mode (at 213 cm^{-1}) normalized to the A_1 mode (at 202 cm^{-1}) is strongly correlated to the degree of broken-site chemical order of the glass network.

Given that the broken-site chemical order in g-GeS_2 (of $29\pm2\%$) is substantially larger than in g-$GeSe_2$ ($16\pm1\%$), and given that the normalized scattering strength of the A_1^c mode provides a measure of broken-bond disorder,[20,29] one would predict the scattering strength ratio A_1^c/A_1 for g-GeS_2 to be larger than in g-$GeSe_2$. Experimentally just the reverse is found provided the 340-cm^{-1} band is assumed to represent scattering from the A_1 band alone. Clearly the 340-cm^{-1} band must have contributions that arise both from the ordered (Ge—S) as well as the disordered (Ge—Ge) bonds with the important consequence that the scattering strength ratio $I(375\ cm^{-1})/I(340\ cm^{-1})$ underestimates the A_1^c/A_1 mode strength ratio.

On the basis of Eq. (3), which describes phase separation of g-GeS_2 into the acceptor (A) and donor (B) clusters, one expects three chemically disordered Ge—Ge bonds (from B cluster) for every 76 chemically ordered Ge—S bonds (from A and B clusters) to be present in the network. This then leads to a broken-bond chemical order of about 4%. If one assumes *a priori* that the Raman scattering cross sections for A_{1g} mode of ethanelike units and the A_1 mode of $Ge(S_{1/2})_4$ tetrahedral units are the same, then one would expect about 5% of the scattering strength of the 340-cm^{-1} mode (in Fig. 6) to derive from the chemically disordered bonds, with the remainder coming from the chemically ordered bonds.

Our discussion here brings out the pivotal role played by Mössbauer spectroscopy in the context of glass structure. In this site spectroscopy one is able to discriminate between the two types of building blocks because the local symmetry of the cations are radically different. The symmetry is tetrahedral in $Ge(S_{1/2})_4$ units leading to a vanishing EFG, while it is trigonal in $Ge_2(S_{1/2})_6$ units leading to a finite EFG.

E. Molecular structure of g-GeS_2: comparison with other experiments

It is instructive to pose the question — in what way do the present conclusions on the structure of g-GeS_2 compare with results of previous experiments on the subject? The picture of molecular phase separation into an A (S-rich) and B (Ge-rich) cluster developed in this work differs qualitatively from a number of previous structure discussions[1,4,8,14] of this glass based on Raman scattering. The Mössbauer evidence of a substantial broken-site chemical order is *qualitatively incompatible* with chemically ordered 3D continuous random networks of g-GeS_2. On the other hand, several workers in recent years have

suggested that the network morphology of g-GeS_2 is not 3D but in fact 2D, and bears a close analogy to the layered structure of β-GeS_2. The pressure-induced optical edge shift experiments of Weinstein *et al.*[30] have shown that the glass structure is more compatible with the 2D rather than the 3D crystalline modification of GeS_2. Other workers, notably Kawamoto and Kawashima,[15] arrived at a similar conclusion by comparing the general shape of the Raman scattering of g-GeS_2 with those of a suitably broadened version of 2D and 3D crystalline modifications of GeS_2.

Murase and co-workers[13] were one of the first to recognize the signature of chemically disordered bonds (S—S) in Raman scattering. Specifically, their vibrational density-of-states calculations in characteristic clusters showed that the 440-cm^{-1} mode in g-GeS_2 can be identified with the S—S stretch of S dimers present at the edge of outrigger raft clusters. These calculations also demonstrated that the corresponding Se—Se stretch mode in g-$GeSe_2$ occur at 247 cm^{-1} and are much weaker in strength in Raman scattering. On this basis Murase and co-workers[13] suspected that the concentration of chalcogen—chalcogen bonds in g-GeS_2 is larger than in g-$GeSe_2$, an indication that the size of chalcogen-rich clusters in g-GeS_2 is smaller than in g-$GeSe_2$. The present experimental results confirm and extend these ideas on molecular phase separation by identifying the size of chalcogen-rich clusters in the two stoichiometric glasses.

X-ray structure factor measurements of Cervinka and Hruby[31] on g-Ge_xS_{1-x} alloys have revealed several significant trends. An anomalous first sharp diffraction peak (FASDP) is observed at approximately 1.1 Å^{-1}. The intensity of the FASDP is found to be a maximum at $x=\frac{1}{3}$ and it decreases when $x>\frac{1}{3}$ or $x<\frac{1}{3}$. Furthermore, these workers also found that the average Ge—S bond length and coordination number [deduced from the radial distribution functions (RDF's)] increase when $x>\frac{1}{3}$. These trends in a general way are precisely the ones one would expect from the present model of molecular phase separation. At the stoichiometric composition $x=0.333$, the concentration of the A microphase is a maximum. Several interpretations have been advanced for the FASDP, including the possibility[32] that it represents a physical correlation length of ~ 6 Å corresponding to the interlayer Ge-Ge separation of the 2D modification of c-GeS_2. Such an interpretation is appealing because it is compatible with the notion that the A molecular cluster in g-GeS_2 represents a molecular fragment of 2D c-GeS_2. The fact that this fragment has been reconstructed at the edges is also supported by measurements of the Mössbauer EFG tensor[20] as well as vibrational spectroscopy.[13]

In the Ge-rich glasses growth of C molecular clusters at the expense of A and B molecular clusters (Fig. 4) provides a natural explanation for an increased coordination number and Ge—S bond lengths. One has merely to recall that in the C molecular cluster Ge has a distorted octahedral coordination.[21] The average Ge—S bond length in this ionic structure is, in general, larger[17] than the one encountered in the more covalently bonded A molecular structure where the cations are tetrahedrally coordinated.

In summary, it appears that the more recent interpretation of Raman scattering experiments, the pressure-induced optical edge shifts, the diffraction experiments, and the current Mössbauer experiments all reinforce the view that g-GeS_2 is phase separated on a molecular scale. The manner in which this phase separation evolves as a function of Sn isovalent atom alloying in pseudobinary $(GeS_2)_{1-x}(SnS_2)_x$ glasses has also been studied and is discussed elsewhere.[33]

V. CONCLUSIONS

Homogeneous melt-quenched $(Ge_{0.99}Sn_{0.01})_xS_{1-x}$ glasses have been prepared over the glass-forming range $0<x<0.43$ and studied by scanning calorimetry, Mössbauer, and Raman spectroscopy. Two distinct and chemically inequivalent ^{119}Sn sites (A and B) are observed at the stoichiometric composition $x=\frac{1}{3}$ with the site intensity ratio $I_B/(I_B+I_A)=0.29(2)$. This ratio is found to vanish at $x<0.325$, and furthermore to change drastically with composition once $x>\frac{1}{3}$. These sites are identified with the presence of Sn dopants replacing Ge sites in two distinct molecular clusters: a layeredlike cluster (A) possessing an internal morphology that resembles c-GeS_2 and a cluster (B) that consists of ethanelike $Ge_2(S_{1/2})_6$ units. The lateral size of the A cluster suggested by these experiments is found to be approximately 30 Å. The 340-cm^{-1} Raman band observed in g-GeS_2 is identified as having scattering contributions from both ordered bonds: the A_1 symmetric stretch of $Ge(S_{1/2})_4$ units; and disordered bonds: the A_{1g} mode of $Ge_2(S_{1/2})_6$ units; the size of the A molecular cluster in g-GeS_2 is a factor of 2 smaller than in g-$GeSe_2$, and this accounts for the substantially larger broken chemical order in GeS_2 glass [0.29(2)] compared to $GeSe_2$ glass [0.16(1)]. In general, it appears that Se-containing glasses polymerize more than their S counterpart. The notion of molecular phase separation in g-GeS_2 is not surprising. After all, it merely represents an extention of the idea so well known in S-rich glasses to the case of the stoichiometric composition.

In the Ge-rich ($x>\frac{1}{3}$) glasses, a third type of a site (C) is observed and identified with a layerlike cluster whose internal morphology resembles that of c-GeS. The 250-cm^{-1} Raman band, whose strength is correlated to the Mössbauer C site intensity, is identified as a double-layer breathing mode of such a cluster.

The sudden loss of bulk glass-forming tendency in both Ge_xS_{1-x} and Ge_xSe_{1-x} glasses, once x exceeds 0.43, can be traced to the presence of the rigid C clusters which become the majority clusters and these clusters percolate. Such clusters are less amenable to surface and edge reconstruction. The rigidity of the C clusters derives from the fact that in this cluster both the anions and cations do not conform to the $8N$ coordination rule.

ACKNOWLEDGMENTS

During the course of this work we have benefitted from valuable discussions with Professor H. R. Chandrasekhar and Dr. Jim Griffiths. This work was supported by the U. S. National Science Foundation under grant No. DMR-82-17541 to the University of Cincinnati.

[1]G. Lucovsky, J. P. deNeufville, and F. L. Galeener, Phys. Rev. B **9**, 1591 (1974); G. Lucovsky, G. L. Galeener, R. C. Keezer, R. H. Geils, and H. A. Six, *ibid.* **10**, 5134 (1974).

[2]M. Tenhover, M. A. Hazle, and R. K., Grasselli, Phys. Rev. B **29**, 6732 (1984); see also J. E. Griffiths, M. Malyj, G. P. Espinosa, and J. P. Remeika, *ibid.* **30**, 6978 (1984).

[3]M. B. Meyers and E. J. Felty, Mater. Res. Bull. **2**, 535 (1967); A. T. Ward, J. Phys. Chem. **72**, 4133 (1968); T. Mori, K. Matsuiski, and T. Arai, J. Non-Cryst. Solids **65**, 269 (1984).

[4]R. J. Nemanich, G. A. N. Connell, T. M. Hayes, and R. A. Street, Phys. Rev. B **18**, 6900 (1978); G. Lucovsky, F. L. Galeener, R. H. Geils, and R.C. Keezer, in *Structure of Non-Crystalline Material,* edited by P. H. Gaskell (Cambridge University Press, Oxford, 1977), p. 127.

[5]P. M. Bridenbaugh, G. P. Espinosa, J. E. Griffiths, J. C. Phillips, and J. P. Remeika, Phys. Rev. B **20**, 4140 (1979); see also K. Murase, T. Fukunaga, K. Yakushiji, T. Yoshimi, and I. Yunoki, J. Non-Cryst. Solids **59-60**, 883 (1983).

[6]P. Boolchand, in *Physical Properties of Amorphous Materials,* edited by D. Adler, B. B. Schwartz, and M. C. Steele (Plenum, New York, 1985), p. 221.

[7]P. Boolchand, J. Grothaus, W. J. Bresser, and P. Suranyi, Phys. Rev. B **25**, 2975 (1982); see also P. Boolchand and J. Grothaus, in *Proceedings of the 17th International Conference on the Physics of Semiconductors, San Francisco, 1984,* edited by J. C. Chadi and W. A. Harrison (Springer-Verlag, New York, 1985), p. 833.

[8]G. Lucovsky, R. J. Nemanich, and F. L. Galeener, in *Proceedings of the 7th International Conference on Amorphous and Liquid Semiconductors, Edinburgh, Scotland, 1977,* edited by W. E. Spear (G. G. Stevenson, Dundee, Scotland, 1977), p. 125.

[9]K. Sisson and P. Boolchand, Nucl. Instrum. Methods **198**, 317 (1982).

[10]P. Boolchand, J. Grothaus, and J. C. Phillips, Solid State Commun. **45**, 183 (1983).

[11]P. Boolchand and Mark Stevens, Phys. Rev. B **29**, 1 (1984).

[12]J. E. Griffiths, J. C. Phillips, G. P. Espinosa, J. P. Remeika, and P. M. Bridenbaugh, Phys. Status Solidi B **122**, K11 (1984).

[13]K. Murase, T. Fukunaga, Y. Tanaka, K. Yakushiji, and I. Yunoki, Physica **117&118B**, 962 (1983). T. Fukunaga, Ph.D. thesis, Osaka University, Japan, 1982 (unpublished).

[14]K. Arai, N. Koshizuka, and H. Namikawa, in *Structure and Excitation on Amorphous Solids (Williamsburg, Virginia, 1976),* proceedings of the conference, edited by G. Lucovsky and F. L. Galeener (AIP, New York, 1976), Vol. 31, p. 217.

[15]Y. Kawamoto and C. Kawashima, Mater. Res. Bull. **17**, 1511 (1982).

[16]Y. Kawamoto and S. Tsuchihashi, J. Am. Ceram. Soc. **52**, 626 (1969); **54**, 131 (1971); see also L. Tichý, N. Ryšavá, A. Tríska, H. Ticha, and J. Klikorka, Solid State Commun. **49**, 903 (1984).

[17]L. Pauling, *The Nature of the Chemical Bond* (Cornell University Press, Ithaca, 1960).

[18]J. C. Phillips and M. F. Thorpe, Solid State Commun. **53**, 699 (1985); M. F. Thorpe J. Non-Cryst. Solids **57**, 355 (1983).

[19]J. C. Phillips, J. Non-Cryst. Solids **34**, 153 (1979); **43**, 37 (1981).

[20]W. J. Bresser, P. Boolchand, P. Suranyi, and J. P. deNeufville, Phys. Lett. **46**, 1689 (1981); W. J. Bresser, P. Boolchand, P. Suranyi, and J. Hernandez (unpublished).

[21]J. Burgeat, G. LeRoux, and A. Brenac, J. Appl. Cryst. **8**, 325 (1975). See also N. Kh. Abrikosov, V. F. Bankina, L. V. Poretskaya, L. E. Shelimova, and E. V. Skudnove, in *Semiconducting II-IV, IV-VI, and V-VI Compounds* (Plenum, New York, 1969), Chap. II. A new high-temperature cubic phase of GeS has been identified by L. K. Vodopyanov, L. V. Golubev, L. Yu Kengerlinskii, and D. I. Bletskan, Fiz. Tverd. Tela (Leningrad) **24**, 1562 (1982) [Sov. Phys.—Solid State **24**, 897 (1982)].

[22]A. Feltz, H. Aust, and A. Blayer, J. Non-Cryst. Solids **55**, 179 (1983).

[23]J. D. Wiley, W. J. Buckel, and R. L. Schmidt, Phys. Rev. B **13**, 2489 (1976).

[24]H. R. Chandrasekhar and U. Zwick, Solid State Commun. **18**, 1509 (1976); and private communication.

[25]H. R. Chandrasekhar, R. G. Humphreys, U. Zwick, and M. Cardona, Phys. Rev. B **15**, 2177 (1977); see also H. R. Chandrasekhar, R. G. Humphreys, and M. Cardona, *ibid.* **16**, 2981 (1977).

[26]R. Zallen, M. L. Slade, and A. T. Ward Phys. Rev. B **3**, 4257 (1971).

[27]See Ref. 8 and also discussion at the end of Ref. 14.

[28]B. A. Weinstein and M. L. Slade, in *Optical Effects in Amorphous Semiconductors (Snowbird, Utah, 1984),* edited by P. C. Taylor and S. G. Bishop (AIP, New York, 1984), p. 457; see also B. A. Weinstein and R. Zallen, in *Light Scattering in Solids IV,* Vol. 54 of *Topics in Applied Physics,* edited by M. Cardona and G. Guntherodt (Springer, New York, 1984), p. 465.

[29]Mark Stevens, P. Boolchand, and J. G. Hernandez, Phys. Rev. B **31**, 981 (1985).

[30]B. A. Weinstein, R. Zallen, M. I. Slade, and J. C. Mikkelsen, Phys. Rev. B **25**, 781 (1982).

[31]L. Cervinka and H. Hruby, in *Amorphous and Liquid Semiconductors,* edited by J. Stuke and W. Brenig (Taylor and Francis, London, 1974), p. 431. See also L. Cervinka, in *The Structure of Non-Crystalline Materials, 1982,* edited by P. H. Gaskell, J. M. Parker, and E. A. David (Taylor and Francis, New York, 1983), p. 255.

[32]J. C. Phillips, in *Proceedings of the 17th International Conference on the Physics of Semiconductors, San Francisco, 1984,* edited by J. C. Chadi and Walter A. Harrison (Springer-Verlag, New York, 1985), p. 775.

[33]J. Grothaus and P. Boolchand, J. Non-Cryst. Solids **72**, 1 (1985).